

# Modeling and Tip Position Control of a Flexible Link Robot: Experimental Results

## *Modelación y Control de Posición del Extremo de un Robot de Eslabón Flexible: Resultados Experimentales*

Juan Fernando Peza Solís, Gerardo Silva Navarro and Rafael Castro Linares

Centro de Investigación y de Estudios Avanzados del I.P.N.

Departamento de Ing. Eléctrica, Sección de Mecatrónica

Av. Instituto Politécnico Nacional 2508. 07360 México D.F., México

jpeza@cinvestav.mx, gsilva@cinvestav.mx, rcastro@cinvestav.mx

*Article received on March 10, 2008; accepted on September 04, 2008*

### **Abstract:**

This work describes the modeling and control of an experimental platform associated to a single link flexible robot, whose motion is restricted to an horizontal plane, thus neglecting the gravity effects. The modeling problem is addressed using the so-called *Euler-Bernoulli* beam equation. The design, construction and integration of an experimental set-up developed for this work is also presented. Two main control schemes are then devised for controlling the end tip position of the flexible link, the passive velocity feedback and strain feedback approaches. Finally, the overall system performance is illustrated by some experimental results obtained with both control methods.

**Keywords:** Flexible link, Modal coordinates, Passivity based control, Strain feedback.

### **Resumen:**

En este trabajo se describe la modelación y control de una plataforma experimental de un robot con un eslabón flexible, cuyo movimiento se restringe a un plano horizontal. El eslabón flexible es una viga larga de acero con poco espesor, por lo que su ecuación de movimiento se obtiene a partir de la ecuación de *Euler-Bernoulli*, que describe a un sistema con masa y rigidez distribuida a lo largo de su coordenada espacial (longitud). Se describe el diseño, construcción e integración de la plataforma experimental. Para los propósitos de control de la posición del extremo libre se aplican dos esquemas de control, el enfoque basado en la retroalimentación pasiva de la velocidad y otro enfoque reciente conocido como retroalimentación del esfuerzo. Finalmente, el desempeño dinámico del sistema en lazo cerrado se ilustra mediante algunos resultados experimentales.

**Palabras clave:** Control basado en pasividad, Eslabón flexible, Coordenadas modales, Retroalimentación de esfuerzo.

## **1 Introduction**

The control of flexible link robots has been widely studied in recent years and there are different models available in the literature [1,3,7,9,10]. A thin and flexible link is described by partial differential equation, highly nonlinear and with complex dynamics, hence, it represents an interesting control problem for the asymptotic output tracking in presence of vibrations. Most of the models are derived from the so-called Euler-Bernoulli equation [8], which is a second order partial differential equation in the time variable and of fourth order in the spatial coordinate. The solution for this equation represents the deflection of the link at a given distance from the selected reference frame as a function of time [7]. In general, the solution is obtained using the modal approach, in which the solution is assumed to be a combination of spatial functions called mode shapes weighted by time functions referred to as modal coordinates. The mode shapes depend on the boundary conditions. In the present paper, clamped-free boundary conditions are used to derive the mode shapes. The mode shapes (vibration modes) are related to a respective natural frequency of the link [8], which in turn, depends entirely on the mechanical parameters of the link.

In order to design an effective control scheme for the end tip of the flexible link, the election of an adequate output is of great importance [9, 10]. Typical results often use a combination of the rotation of the motor shaft (referred to as rigid mode) plus the deflection of the link at the tip. In this way, an output expression for the total tip

deflection, measured from a fixed reference frame was obtained. However, controllers proposed for such an output were found to be complicated. In this context, it is known that using the rotation of the motor plus the reflected deflection of the tip, to the rigid mode, as an output function, leads to a transfer function with a well defined relative degree [10]. Then, a passive output, which relates the input link torque, applied by the motor, to the angular velocity of the end tip, can be used in combination with a strictly passive compensator to stabilize the overall system [9, 10].

In this paper it is considered the regulation and tracking control problem of the end tip position of one flexible link, actuated by a DC motor and excited up to its first three flexible modes, in contrast to most of the existing results for one mode deflection and slow motions (low frequency components). The mathematical model includes the dynamics of these three modes, with beam deflections estimated via three strain gages, and the dc motor. Two different control schemes (passive velocity feedback and strain feedback) are applied to an experimental setup, both resulting in good dynamic behaviors.

## 2 Modeling

### System description

The flexible link considered in this work consists of a rotating flexible link whose base is clamped to a DC motor shaft, as shown in figure 1.

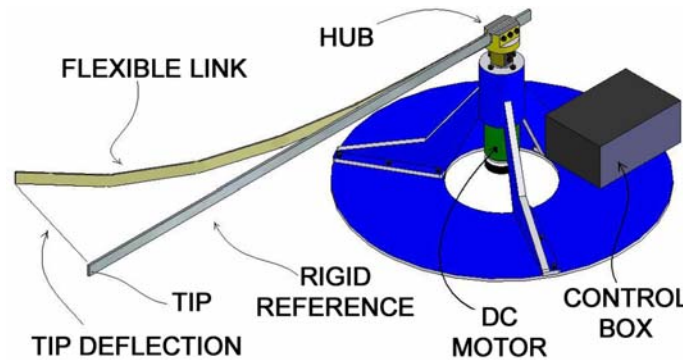


Fig. 1. Flexible link robot set-up

The flexible link is a thin metallic beam which is attached to move around the motor shaft in an horizontal plane; the elastic deflection of the link takes place in the same motion plane, so that the gravity effects can be neglected. The link is a uniform aluminum beam of  $0.003175m \times 0.0254m \times 1m$  and the actuator of the system is a DC motor which generates the input torque to the link. The angular displacement of the rigid mode is measured via an optical encoder directly attached to the motor shaft, and the modal coordinates are estimated using a set of strain gages attached at specific positions along the link. A detailed description of the flexible beam built can be found in [7].

### Modeling of the flexible link

The flexible link is considered to be a uniform beam of length  $L$ , with a constant transverse section  $A$ , the cross-section moment of inertia is  $I_A$ , and a uniform mass distribution  $\rho$ . The beam stiffness  $EI_A$  is also taken to be a constant. Since no external force distributions are applied in this case, the Euler-Bernoulli equation is simplified to

$$\rho A \frac{\partial^2 w}{\partial r^2}(r, t) + EI_A \frac{\partial^4 w}{\partial r^4}(r, t) = 0 \quad (1)$$

where  $r$  is the spatial coordinate,  $t$  is the time and  $w(r,t)$  represents the deflection of the beam from a reference frame, which is attached to the base of the link. A solution for (1) can be obtained using the assumed-modes approach, in which the deflection is expressed by

$$w(r,t) = \sum_{i=0}^{\infty} q_i(t)\varphi_i(r) \tag{2}$$

where  $\varphi_i(r)$  represents mode shapes and  $q_i(t)$  denotes the modal coordinates. The clamped-free boundary conditions are given by

$$\begin{aligned} \varphi_i(0) = 0, \quad \frac{d\varphi_i}{dr}(0) = 0 \\ \frac{d^2\varphi_i}{dr^2}(L) = 0, \quad \frac{d^3\varphi_i}{dr^3}(L) = 0 \end{aligned} \tag{3}$$

The first three mode shapes for a clamped-free beam are depicted in figure 2. For faster motion of the DC motor shaft (see figure 1) more vibration modes can be excited and, as consequence, the position control of the end tip position of the flexible link will be more difficult.

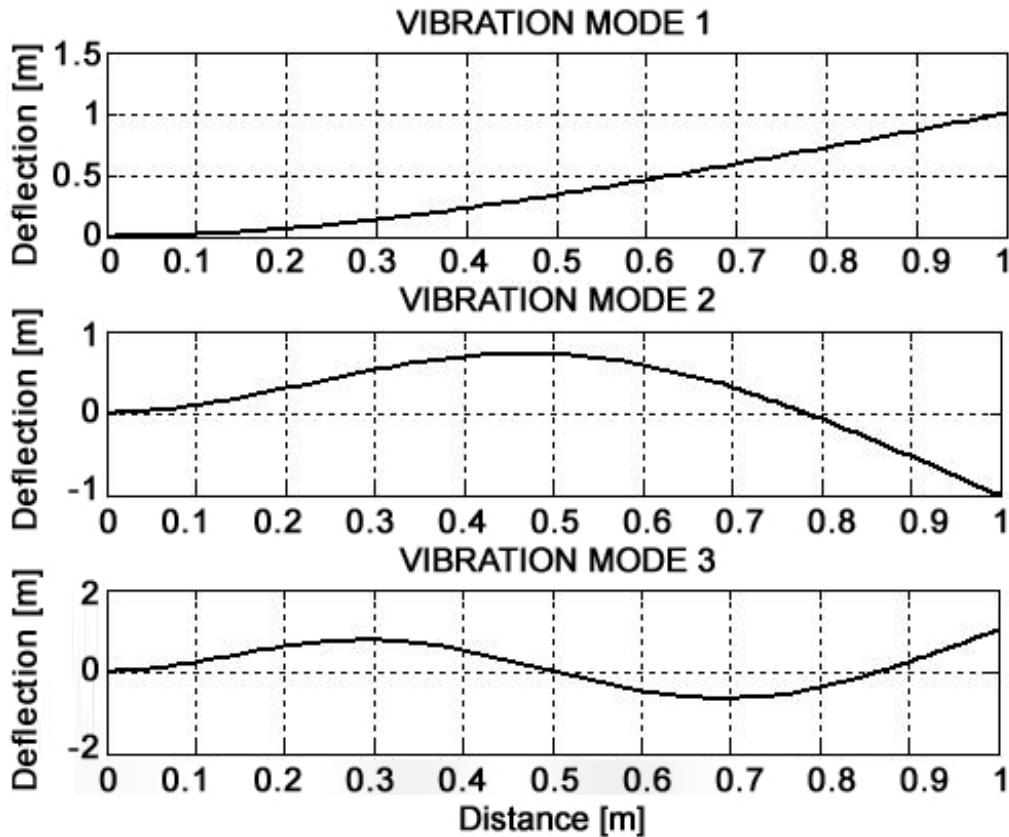


Fig. 2. Clamped-Free modal shapes for a thin beam

Using the mode shapes approach, the model of the rotating flexible link can be expressed as

$$EI_A \frac{\partial^4 w}{\partial r^4} + \rho A \frac{\partial^2 w}{\partial t^2} = -\rho A [(r + R)\ddot{\theta} - w\dot{\theta}^2] \quad (4)$$

where  $R$  represents the coupling shaft radius. Due to the fact that the link is restricted to move on an horizontal plane, no gravity terms are included. Besides, the term  $w\dot{\theta}^2$  in (4) is also neglected due to the real dimensions of the experimental platform (see, for example, [2,7]). Thus, the model (4) takes the form

$$EI_A \frac{\partial^4 w}{\partial r^4} + \rho A \frac{\partial^2 w}{\partial t^2} = -\rho A [(r + R)\ddot{\theta}] \quad (5)$$

Since the mode shapes and boundary conditions are known, they can be applied to (5) resulting in the following set of second order linear differential equations,

$$\ddot{q}_i(t) + \omega_i^2 q_i(t) = M_i \ddot{\theta}(t), \quad i = 1, 2, \dots \quad (6)$$

where

$$M_i = \frac{R\beta_i + \gamma_i}{\alpha_i}, \quad i = 1, 2, \dots \quad (7)$$

with

$$\alpha_i = \int_0^L \varphi_i^2(r) dr, \quad \beta_i = \int_0^L \varphi_i(r) dr, \quad \gamma_i = \int_0^L r \varphi_i(r) dr$$

Let us now consider that the coupling shaft inertia is  $I_h$ , the shaft rotation angle is  $\theta$ , and the flexible link mass distribution along its length is concentrated in its centre of gravity (CG). The CG is out of the deflection curve when the link is deflected, so that a way to express its relative position to the rotating reference frame attached to the base of the link must be found. Recalling that the deflection curve  $w(r, t)$  is the solution for the *Euler-Bernoulli* equation, making basic geometric considerations and carrying out some straightforward calculations, it can be shown that the position of the CG of the deflected beam  $(L/2, w_c)$ , relative to the reference frame attached to the base of the link, can be expressed in terms of the mode shapes as

$$w_c(t) = \frac{1}{L} \sum_{i=1}^n q_i(t) \int_0^L \varphi_i(r) dr \quad (8)$$

According to figure 3, the rotation angle of the CG of the link, denoted as  $\psi(t)$  and measured from the fixed reference frame, is a composed quantity given by

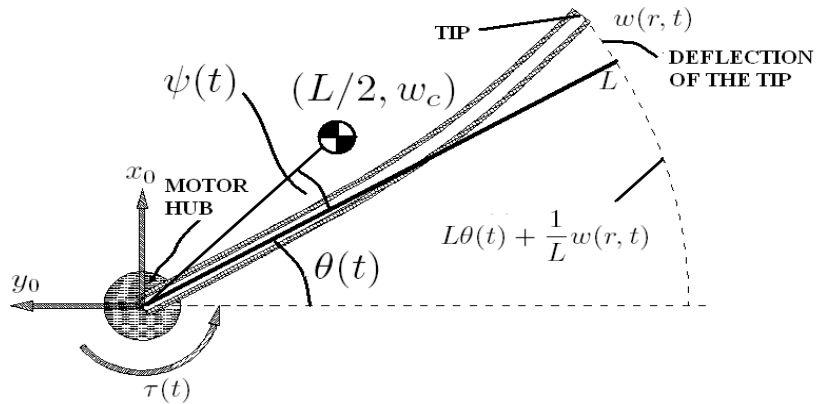


Fig. 3. Flexible link layout

$$\psi(t) = \theta(t) + \frac{2}{L^2} \sum_{i=1}^n \mu_i q_i(t) \tag{9}$$

where  $\mu_i$  is a constant denoting the integral of the  $i$ -th flexible mode in (8). Thus, the kinetic energy of the whole system can be expressed as

$$E_k = \frac{1}{2} I_h \dot{\theta} + \frac{1}{8} \rho A L^3 \left[ \dot{\theta} + \frac{2}{L^2} \sum_{i=1}^n \mu_i \dot{q}_i \right]^2 \tag{10}$$

and the potential energy of the system is given by

$$E_p = \frac{1}{2} \sum_{i=1}^n \frac{\omega_i^2}{\Omega_i} q_i^2 \tag{11}$$

where  $\Omega_i = |N_i|$  and  $N_i = \frac{2M_i}{\rho A L^3}$ . Defining  $\mathbf{L} = E_k - E_p$  as the lagrangian function for this system, where  $\psi$  and the  $q_i$ 's, for  $i = 1, \dots, n$ , are the generalized coordinates, the Euler-Lagrange dynamic equations for the system take the form

$$\left[ I_h + \frac{1}{4} \rho A L^3 \right] \ddot{\theta} + \frac{1}{2} \rho A L \sum_{i=1}^n \mu_i \ddot{q}_i = \tau \tag{12}$$

and for the  $i$ -th flexible mode one has that

$$\frac{1}{2} \rho A \mu_i \left[ \ddot{\theta} + \frac{2}{L^3} \sum_{j=1}^n \mu_j \ddot{q}_j \right] + \frac{\omega_i^2}{\Omega_i} q_i = 0 \tag{13}$$

By multiplying (13) by  $\dot{q}_i$ , and carrying out a summation for the  $n$  flexible modes, it can be shown that

$$\sum_{i=1}^n \frac{\omega_i^2}{\Omega_i} q_i \dot{q}_i = -\frac{1}{2} \rho A L \ddot{\theta} \sum_{i=1}^n \mu_i \dot{q}_i - \frac{\rho A}{L} \sum_{i=1}^n \mu_i \dot{q}_i \sum_{i=1}^n \mu_i \ddot{q}_i \quad (14)$$

The left hand member of (14) is just  $\dot{E}_p$ . Thus,  $E = E_k + E_p$  and using (12) one has that

$$\dot{E} = \tau \dot{\theta} + \frac{1}{2} \rho A L \ddot{\theta} \sum_{i=1}^n \mu_i \dot{q}_i + \frac{\rho A}{L} \sum_{i=1}^n \mu_i \dot{q}_i \sum_{i=1}^n \mu_i \ddot{q}_i + \dot{E}_p \quad (15)$$

therefore, the substitution of (14) into (15) yields

$$\dot{E} = \dot{E}_k + \dot{E}_p = \tau \dot{\theta} \quad (16)$$

which holds up to  $n$  flexible modes. Thus, the system model satisfies the energy conservation property. It should be noticed, however, that some viscous damping is present in the physical system.

### 3 Passivity-based control of the end effector

#### Derivation of a passive transfer function

For control purposes, it is necessary to propose an adequate output function. Such an output is crucial, since this makes possible to design a simple controller with acceptable results; in fact, a bad choice of the output function can lead to system instability.

In the following,  $q_0(t)$  is the rigid mode ( $\theta(t)$  in this case),  $q_i(t)$  is the set of modal coordinates for the flexible link, and  $n$  is the total number of modes considered in the model.

The dynamics for the rigid mode (rotational degree of freedom) is given by

$$\left[ I_h + \frac{1}{2} \rho A L^3 \right] \ddot{q}_0(t) = \tau(t) \quad (17)$$

For the flexible modes one has

$$\ddot{q}_i(t) + \omega_i^2 q_i(t) = N_i \tau(t), \quad i = 1, 2, \dots \quad (18)$$

where  $I_h$  is the moment of inertia for the motor shaft,  $\frac{1}{2} \rho A L^3$  is the moment of inertia due to the mass of the link at its center of mass,  $\tau(t)$  is the applied torque at the base of the link. Note that  $\tau(t)$  is the control input to the system provided by a DC motor. A more complete model of this system should include the electrical dynamics associated to the DC motor, but this can be neglected because it is faster than the mechanical dynamics of the link and shaft. From the dynamics (17), the transfer function from the input torque  $T(s)$  to the rigid mode  $Q_0(s)$  is easily obtained as

$$\frac{Q_0(s)}{T(s)} = \frac{1}{\left[ I_h + \frac{1}{2} \rho A L^3 \right] s^2} \quad (19)$$

In the same way, a set of transfer functions from  $T(s)$  to the flexible modes  $Q_i(s)$  is calculated from (18) as

$$\frac{Q_i(s)}{T(s)} = \frac{N_i}{s^2 + \omega_i^2}, \quad i = 1, 2, \dots \quad (20)$$

In [10], an artificial output of the system, known as the *reflected output*, is employed to derive a transfer function with a well defined relative degree. This output is, in general, the displacement of the end tip, due to the rotation of a rigid mode minus the elastic deflection of the link, due to the flexible modes. This is opposed to the displacement of the tip, due to the rigid mode, augmented with the elastic deflection, which actually happens. It is important to mention that, the mode shapes used in [10] are the pinned-free functions instead of the clamped-free functions considered here. It was shown in [1] that the two models are equivalent. For the clamped-free beam considered in this work, the reflected output is given by

$$y_{ref}(t) = Lq_0(t) - \sum_{i=1}^n \varphi_i(L)q_i(t) \quad (21)$$

and the resulting transfer function, from the input torque to the reflected output has a relative degree equal to 2. It is also of interest to obtain a transfer function with a relative degree equal to 1. Hence, the transfer function from  $T(s)$  to  $sY_{ref}(s)$  is given by

$$\frac{sY_{ref}(s)}{T(s)} = \frac{L}{(I_h + \frac{1}{2}\rho AL^3)s} - \sum_{i=1}^n N_i \varphi_i(L) \frac{s}{s^2 + \omega_i^2} \quad (22)$$

It is well known that  $1/s$  and  $s/(s^2 + \omega_i^2)$  are both passive. For the transfer function (22) to be passive it is necessary that the coefficients of  $s/(s^2 + \omega_i^2)$  be non-negative [5,6]. However, this is not true, because  $N_i < 0$  and  $\varphi_i(L) = (-1)^{i+1}$  for the clamped-free mode shapes [8]. That is, the coefficients  $N_1\varphi_1(L)$  and  $N_3\varphi_3(L)$  are negative, whereas the coefficient  $N_2\varphi_2(L)$  is positive, and the transfer function (22) is not passive. Therefore, another output function is proposed, more precisely

$$y_{MIR}(t) = Lq_0(t) - \sum_{i=1}^n (-1)^{i+1} k_i \varphi_i(L)q_i(t) \quad (23)$$

Equation (23) is called *the negative mode reflected output*, where  $k_i$  represents a set of positive coefficients referred to as *modal weights*. Due to the fact that  $\varphi_i(L) = (-1)^{i+1}$ , the differentiated transfer function from  $T(s)$  to  $sY_{mr}(s)$  takes the form

$$\frac{sY_{MIR}(s)}{T(s)} = \frac{L}{(I_h + \frac{1}{2}\rho AL^3)s} - \sum_{i=1}^n \frac{k_i N_i s}{s^2 + \omega_i^2} \quad (24)$$

whose coefficients are always positive since  $N_i < 0$  for  $i = 1, 2, \dots, n$ . Thus, the passivity property is obtained by reflecting only the odd mode shapes, which leads to negative coefficients in  $s/(s^2 + \omega_i^2)$  when  $i$  is odd.

#### 4 A passivity-based PID control

A well known result in passivity based control states that, if the compensator in figure 4 is strictly passive with finite gain and the plant is passive, then the closed loop system is  $L_2$ -stable [6, 10].

Since the transfer function (24) is passive, a strictly passive compensator with finite gain will stabilize the overall system. The simplest compensator is given by

$$C(s) = \frac{K_x s}{\frac{s}{\omega_f} + 1} \quad (25)$$

where  $\omega_f$  must be higher than the last natural frequency considered in the model, but lower than the first natural frequency rejected. Compensator (25) stabilizes the system for the output (23) in which the shaft rotation and the deflections effects are combined. After stabilizing the system, via the passive compensator (25), a simple controller can be applied to regulate the tip position. In this work, a classical PID controller is implemented on an external control loop [4] (see figure 4).

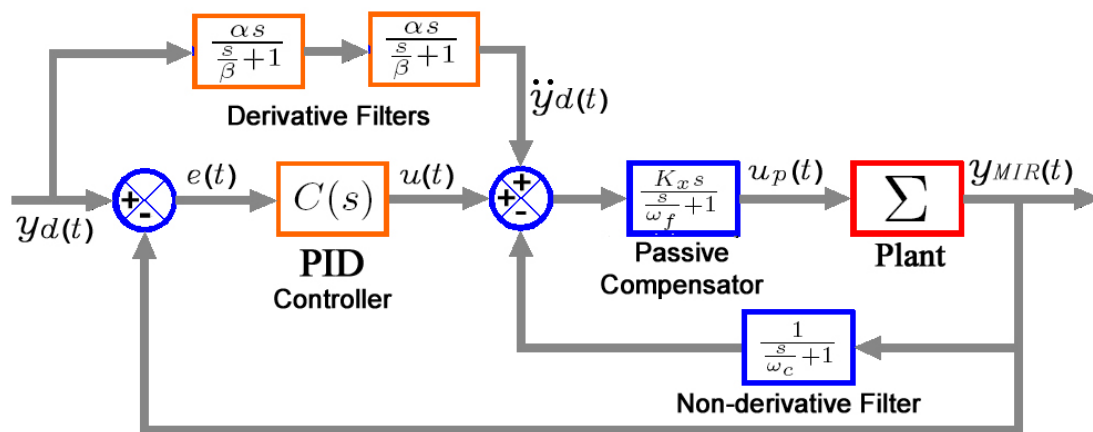


Fig. 4. Passivity-based PID control for trajectory tracking of the tip position

To achieve the trajectory tracking using the above PID controller is included a feed-forward term with the acceleration of the desired reference trajectory (see the two first order filters in figure 4). This compensator yields the approximate acceleration, with an attenuation frequency set by adjustment of the  $\beta = 0.5$  parameter, together with the parameter  $\alpha = 1$ .

#### 5 Strain feedback control

A different control approach for flexible-link robots is the so-called *strain feedback* control [4]. In this case, the main objective of the controller is to regulate the joint position while trying to damp out the flexible-link vibrations, rather than controlling directly the tip position. Measurements of the elastic deflection of the link are taken using a strain gage attached to the link. The voltage signal obtained from the strain gage is, in fact, a measurement of the strain present in the deflected link. It is well known that the strain present in a deflected beam is directly related to its bending moment curve and that the bending moment can be expressed in terms of the elastic deflection of the beam. Therefore, a measurement of the elastic deflection of the link can be obtained by using the voltage signal gathered

from the strain gages. The voltage signal  $V_{sg}$  gathered from the strain gage can be expressed in term of the modal solution as

$$V_{sg}(t) = k_f \sum_{i=1}^{\infty} \varphi_i''(r_s) q_i(t) \quad (26)$$

where  $k_f$  is a scaling constant and  $r_s$  is the position of the strain gage along the link. The control law employed in this scheme then takes the form

$$\tau = -k_p [\theta(t) - \theta_f] - k_v \dot{\theta}(t) - k_f \sum_{i=1}^{\infty} \varphi_i''(r_s) q_i(t) \int_0^t \dot{\theta}(t) \sum_{i=1}^{\infty} \varphi_i''(r_s) q_i(s) ds \quad (27)$$

which is a classic PD controller extended to the flexible case by the addition of an integral term which includes the effects of the elastic deflection in terms of the strain signal sensed by the gage.

In order to verify the closed-loop stability properties for this system, a storage function is chosen as

$$V = E_k + E_p + \frac{1}{2} k_p [\theta(t) - \theta_f]^2 + \frac{1}{2} k_f \left[ \int_0^t \dot{\theta}(t) \sum_{i=1}^{\infty} \varphi_i''(r_s) q_i(s) ds \right]^2 \quad (28)$$

which is a positive definite function. Then, taking the time derivative of (28) yields

$$\dot{V} = \dot{E}_k + \dot{E}_p + k_p \dot{\theta} [\theta - \theta_f] + k_f \dot{\theta} \sum_{i=1}^{\infty} \varphi_i''(r_s) q_i \int_0^t \dot{\theta} \sum_{i=1}^{\infty} \varphi_i''(r_s) q_i(s) ds \quad (29)$$

and, by substituting (16) in (29) one obtains

$$\dot{V} = \tau \dot{\theta} + k_p \dot{\theta} [\theta - \theta_f] + k_f \dot{\theta} \sum_{i=1}^{\infty} \varphi_i''(r_s) q_i \int_0^t \dot{\theta} \sum_{i=1}^{\infty} \varphi_i''(r_s) q_i(s) ds \quad (30)$$

Then, using the control law (27), it can be shown that

$$\dot{V} = -k_v \dot{\theta}^2(t)$$

which is negative semidefinite. Hence, the closed loop system is stable [6]. Notice, however, that the presence of viscous damping in the physical system allows guaranteeing asymptotic stability (see [2] for a detailed discussion of this issue).

## 6 The experimental setup

In order to validate the above results, an experimental platform with a flexible link robot was completely designed, constructed and integrated [2]. The overall system is described in the block diagram shown in figure 5.

The experimental platform has a DC motor to actuate the flexible link at its clamped base. The rotation angle of the motor shaft is measured with an optical encoder attached to the motor shaft. This DC motor was tested and validated, to provide the required control torques.

The elastic deflection of the end tip is measured via a set of three strain gages, which are attached to the flexible link at specific positions to measure the dynamical contribution up to the first three flexible modes. The selection of those locations for the strain gages depends on granting the invertibility property of the so-called *decoupling matrix* [2,7]; this is of utmost importance, since a bad choice in locating the gages can lead to closed-loop system instability. A common placement procedure consists in placing the gages on positions where the strain due to the first rejected flexible mode equals zero [7]. In the present case, the first rejected mode is the fourth one.

The use of strain gages as deflection sensors requires some additional instrumentation circuits and a signal conditioning stage. A set of commercial-available Wheatstone bridges, each one with its respective instrumentation amplifier is employed to gather the information signal from the set of strain gages. The controllers devised for this prototype are implemented into a PC with an acquisition card Sensoray 626, included as a part of the signal conditioning stage in the set-up to provide the D/A and A/D operations, and running under *Windows XP*® and *Matlab/Simulink*® (see figure 5). A photograph of the experimental setup is shown in figure 6.

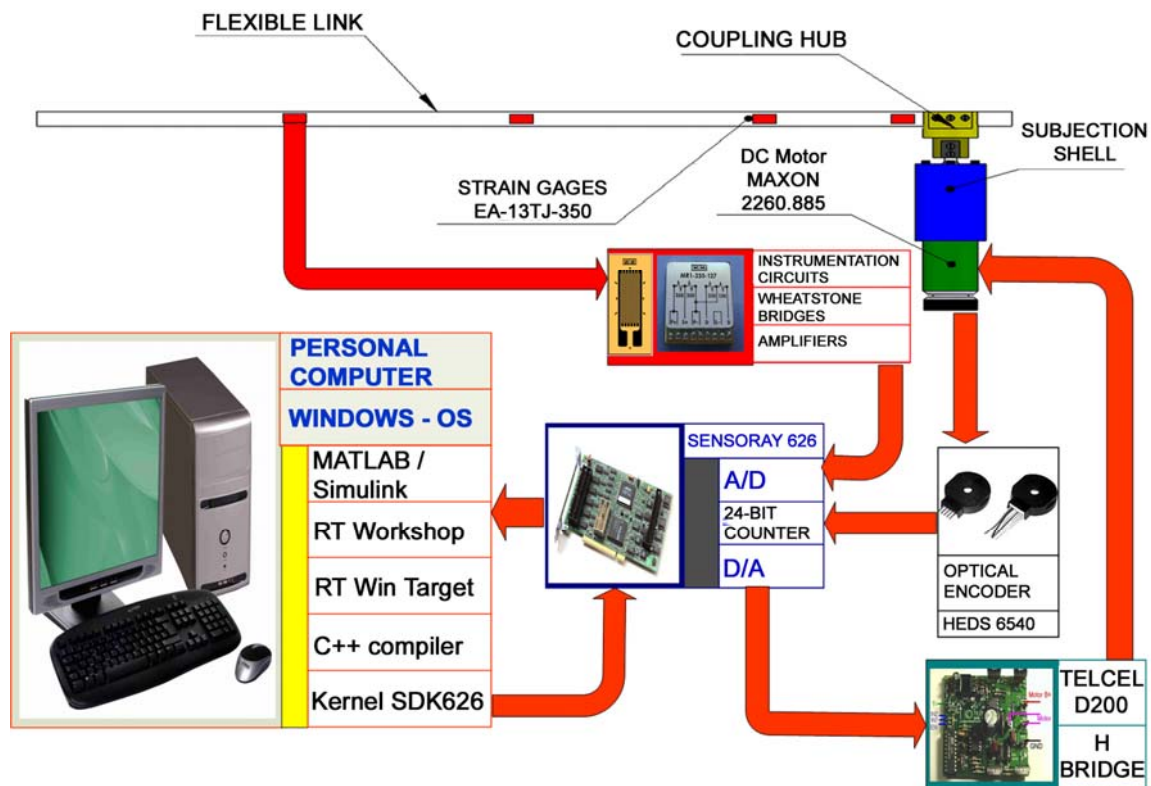


Fig. 5. Schematic diagram of the integration of the experimental set-up

## 7 Experimental results

The physical parameters of the experimental platform are shown in table 1. Some of the parameters in that table are associated to physical dimensions or material properties of the flexible link while others were estimated via several static and dynamical tests [2].

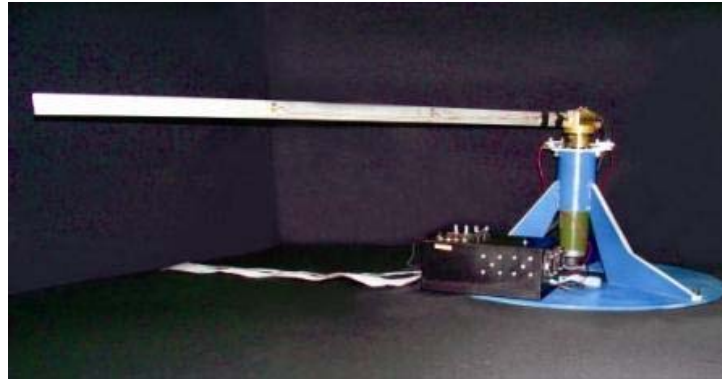


Fig. 6. The experimental platform of the flexible-link robot arm

Table 1. Parameters for the flexible link robot

Parameter	Value	Parameter	Value
$\rho$	$2700 \text{ Kg}/\text{m}^3$	$E$	$68 \text{ GPa}$
$I_A$	$3.20 \times 10^{-10} \text{ m}^4$	$A$	$8.0645 \times 10^{-5} \text{ m}^2$
$I_h$	$27.059 \times 10^{-4} \text{ Kg} \cdot \text{m}^2$	$\omega_1$	$16.1724 \text{ rad}/\text{s}$
$\omega_2$	$101.3511 \text{ rad}/\text{s}$	$\omega_3$	$283.7861 \text{ rad}/\text{s}$
$N_1$	$-10.8799 \text{ 1}/(\text{Kg} \cdot \text{m})$	$N_2$	$-1.9297 \text{ 1}/(\text{Kg} \cdot \text{m})$
$N_3$	$-0.8000 \text{ 1}/(\text{Kg} \cdot \text{m})$	$b_R$	$0.01 (\text{N} \cdot \text{s})/\text{m}$
$\zeta_1$	$0.001 (\text{N} \cdot \text{s})/\text{m}$	$\zeta_2$	$0.001 (\text{N} \cdot \text{s})/\text{m}$
$\zeta_3$	$0.001 (\text{N} \cdot \text{s})/\text{m}$		

**Model performance**

Some numerical simulations of the system were carried out using the parameters shown in table 1 in an open-loop scheme. To obtain the open-loop link behavior, the motor shaft is regulated, without considering the flexural effects of the link, to a desired position, thus allowing the flexible link to bend freely. The validation of the model for the elastic deflection of the link is depicted in figure 7. From that figure a good matching can be observed between the system model and the experimental results, in spite of large beam deflections (about 150 mm).

The amplitude spectrum (FFT) of this experiment is shown in figure 8 where the first three vibration modes of the flexible link occur at 1.98 Hz, 8.6 HZ and 19.07 Hz, respectively.

**Passivity-based PID control results**

Some experimental results for the regulation problem, using the passivity-based PID control scheme, are shown in figure 9. The PID gains were set to  $k_p = 0.25$ ,  $k_v = 0.1$  and  $k_l = 0.01$ , whereas the modal weights were set to  $k_1 = 1$ ,  $k_2 = 1$  and  $k_3 = 1$ ; it should be said that, since there are six control parameters to adjust, the tuning is not an easy task. The upper graphic shows the joint angular position (end effector) of the flexible link when the controlled output is the artificial tip position  $y_{MIR}(t)$ , whereas the lower graphic shows the elastic deflection of the flexible link at the end tip. The last graphic represents the control action applied via the DC motor. From this

experiment one can notice that the tip position achieves the step reference (1.57 rad) in approximately in 2 s, with contributions of the first three flexible modes, significant beam deflections (80 mm) and small control efforts.

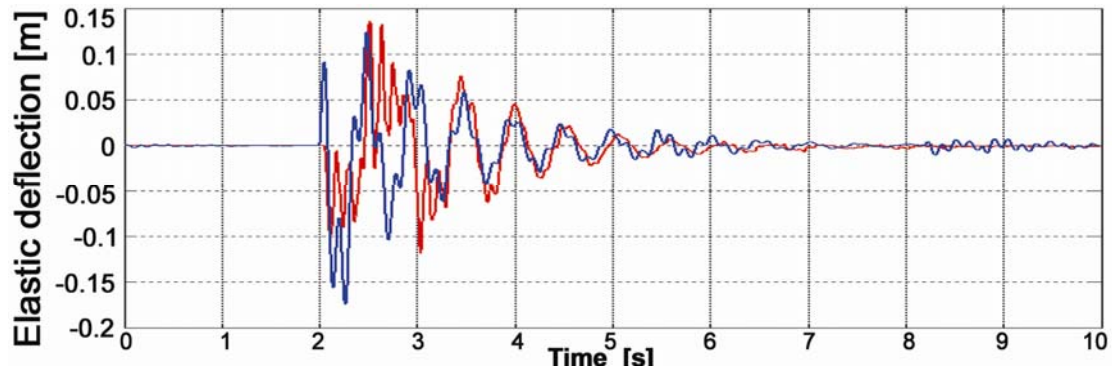


Fig. 7. Experimental validation for the deflection of the tip. Numerical result (blue line) and Experimental result (red line)

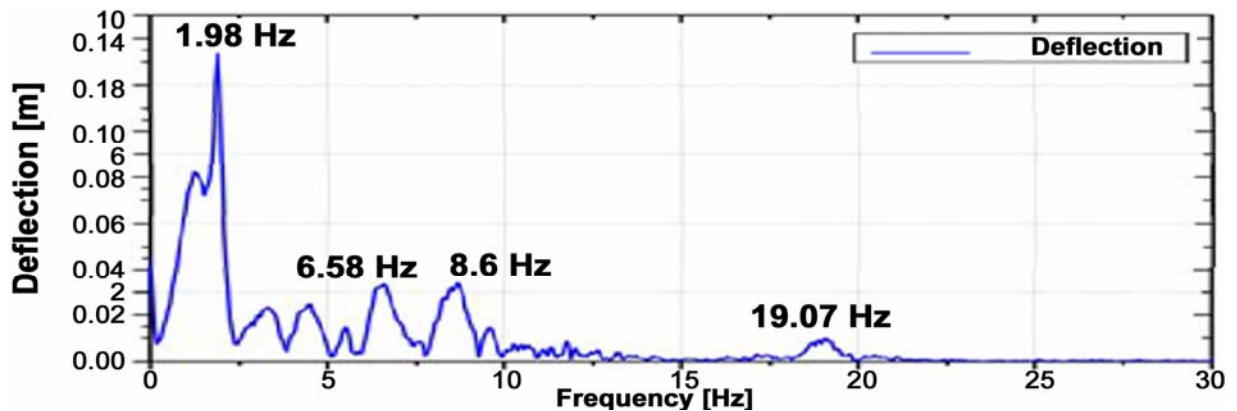


Fig. 8. Amplitude spectrum (FFT) of the flexible link

Additional experimental results for trajectory tracking, when using the passivity-based PID control scheme, are shown in figure 10. The desired trajectory was chosen to be a periodic signal given by  $y_d(t) = 0.2617 \sin(2t)$  [rad]. In this experiment the parameters of the control law were set to  $k_p = 0.25$ ,  $k_v = 0.1$  and  $k_f = 0.01$  and the modal weights to  $k_1 = 3$ ,  $k_2 = 3$  and  $k_3 = 3$ . Figure 10 shows also the elastic deflection at the tip. From the results shown one can notice a good tracking performance with a small phase lag and steady-state errors of 0.015 rad (5.6%), mostly attributed to the presence of backlash in the DC motor.

### Strain feedback control results

Some experimental results for the strain feedback control scheme are shown in figure 11. In this control scheme there are only three control parameters making the tuning of the controller easier when compared to the passivity-based control scheme. For the experiment shown the parameters were set to  $k_p = 0.0000002$ ,  $k_v = 0.0000005$  and  $k_f = 0.0000004$ . The upper graphic represents the joint angular position (end effector) of the flexible link while the lower graphic represents the voltage strain signal gathered from one of the gages attached to the flexible link. The

step reference (1.57 rad) is achieved in approximately 1 s, without overshoot. It is important to remark that this control method is simple and easier to be applied for regulation purposes on flexible links.

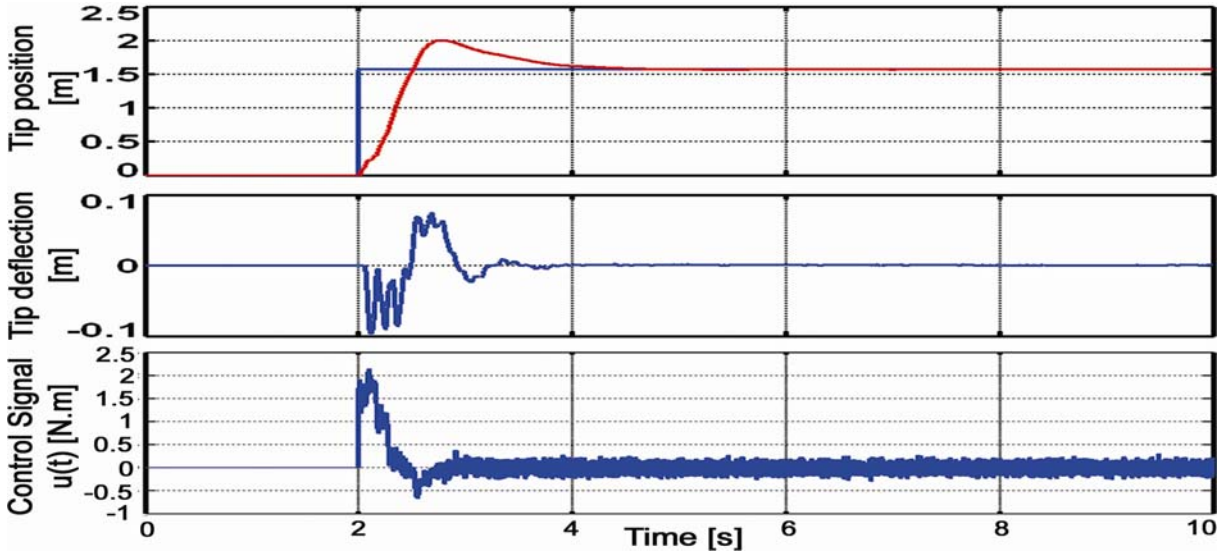


Fig. 9. Experimental results using the passivity-based PID control (regulation). Desired step signal (blue line) and tip position (red line)

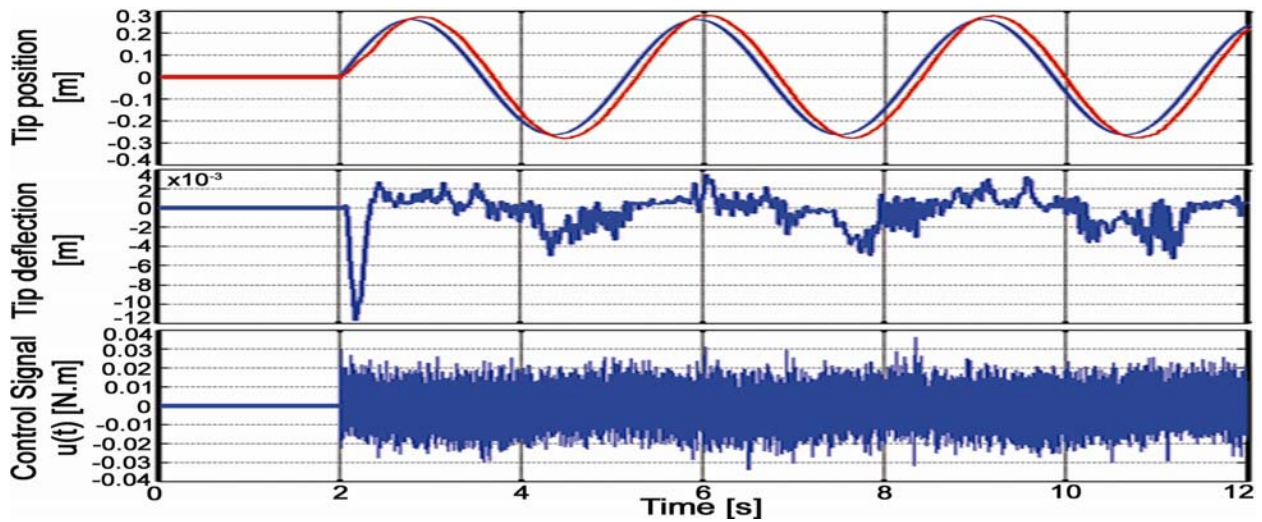


Fig. 10. Experimental results using the passivity-based PID control (trajectory tracking). Desired trajectory (blue line) and tip position (red line)

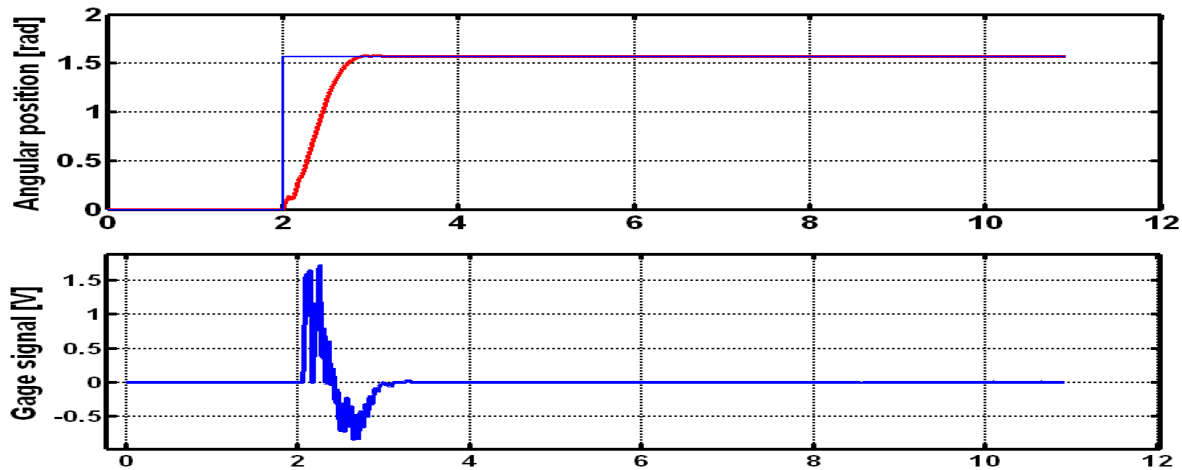


Fig. 11. Experimental results using the strain feedback control (regulation). Desired step signal (blue line) and tip position (red line)

## 8 Conclusions

In this work the modeling and tip position control of a single link flexible robot arm, whose motion is restricted to an horizontal plane, are addressed. It is shown that the negative mode reflected output yields acceptable results, since it makes possible to derive a passive transfer function to stabilize the overall system. The modal weights  $k_i$  provide a way to distribute the energy between the mode shapes, and they can be used also to reduce the vibration effects, but in change, lower vibrations of the flexible modes will increase the rigid mode motion. A passivity based PID control was implemented in order to achieve the asymptotic output tracking for the end tip position, obtaining a good system performance, even when the first three modes of the physical system are being excited. In addition, a strain feedback control scheme was applied to the one flexible link robot, obtaining better results with an easier implementation and tuning.

## References

1. Belleza, F., Lanari, L. and Ulivi, G. "Exact modeling of the slewing link", *Proc. of the IEEE Int. Conf. on Robotics and Automation*, pp. 734-739, Cincinnati, USA, 1990.
2. Peza-Solis, J.F. *Design, construction, modelling and control of a flexible beam robot arm*, M.Sc. Thesis (in Spanish), CINVESTAV-IPN, Department of Electrical Engineering, Mexico City, Mexico, 2008.
3. Cheong, J. and S, S. "Linear PID composite controller and its tuning for flexible link robots", *J. of Vibration and Control*, 14(3), pp. 291-318, 2008.
4. Ge, S.S., Lee, T.H. and Zhu, G. "Improving regulation of a single-link flexible manipulator with strain feedback", *IEEE Trans. on Robotics and Automation*, 14(1), pp. 179-185, 1998.
5. M. Herrera, R. Castro, and Glumineau, A. "Passivity-based control for tip regulation of a flexible beam", *Proc. of the 3rd IASTED, Int. Conf. on Robotics and Manufacturing*, pp. 134-137, Cancún, Q.R., México, 1995.
6. Khalil, H.K. *Nonlinear Systems*, Prentice-Hall, NJ, 1996.
7. Kruijs, L. *Modelling and control of a flexible beam and robot arm*, PhD Thesis, University of Twente, Enschede, The Netherlands, 1990.
8. Meirovitch, L. *Fundamentals of Vibrations*, McGraw-Hill, NY, 1986.
9. Saad, M., Saydy, L. and Akhrif, O. "Noncollocated passive transfer functions for flexible link robot", *Proc. of the IEEE Int. Conf. on Control Applications*, pp. 971-975, Anchorage, Alaska, 2000.

10. Wang, D. and Vidyasagar, M. "Passive control of a stiff flexible link", *The Int. J. of Robotics Research*, 11(6), pp. 572-578, 1992.



**Juan Fernando Peza Solís** was born in Mexico City in 1980. He received a BSc in Mechatronics from UPIITA-IPN, Mexico City, in 2003, and the MSc degree in Electrical Engineering (Mechatronics) from CINVESTAV-IPN, México City, in 2008. He is currently a PhD Student at the Mechatronics Section in CINVESTAV-IPN and his research interests are mechatronic design, flexible robots and vibration control.



**Gerardo Silva Navarro** received the BSc in Mechanical Engineering (1988) and MSc in Electrical Engineering (1990) both from the Instituto Tecnológico de la Laguna (Torreón, México) and his PhD in Electrical Engineering (Automatic Control) in 1994 from CINVESTAV-IPN (México). He is a titular researcher in the Mechatronics Section in CINVESTAV-IPN (México City), with research interests on mechatronics, passive/active vibration absorbers for mechanical systems, rotating machinery, mechanical design and nonlinear control systems.



**Rafael Castro Linares** received the BSc in Communications and Electronics (1981) from the ESIME-IPN (México City), the MSc and PhD both in Electrical Engineering from CINVESTAV-IPN (México City) in 1982 and 1987, respectively. He is currently a titular researcher in the Mechatronics Section in CINVESTAV-IPN. He has been visiting professor in the Laboratoire d'Automatique de Grenoble (Grenoble; France), Università di Roma "La Sapienza" (Rome, Italy), IRCN (Nantes, France), Department of Applied Mathematics of the University of Twente (Enschede, The Netherlands) and the Department of Electrical Engineering of the University of Chile (Santiago, Chile). His research interests are nonlinear control systems, passivity and the applications to robotics and servomechanisms.